Figure S1. Molecular docking of *PNPLA3*_rs738409 (I148) and MT (148M) with a bioactive compound for delphinidin 3-caffeoylglucoside

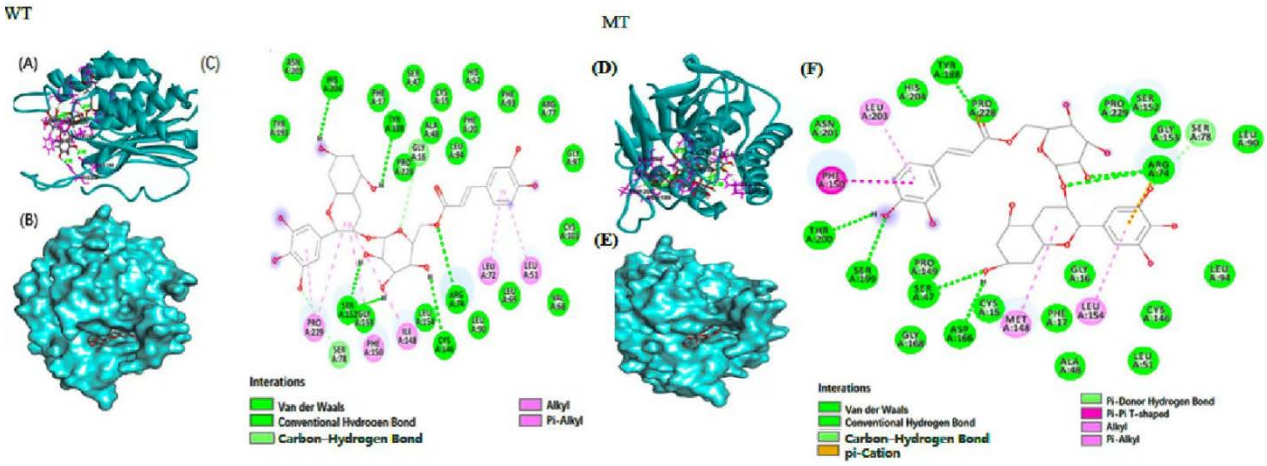

(A,D) Diagrammatic representation of the compound (ball and stick model) binding with WT and MT of *PNPLA3*, respectively. (B,E) binding of the compound at the central cavity with WT and MT of *PNPLA3*, respectively. (C,F) 2D depiction of *PNPLA3* interacting with the compound and the nature of forces involved in stabilizing–complex of bioactive compound WT and MT of *PNPLA3*, respectively. *PNPLA3*, phospholipase domain containing 3.

Figure S2. Molecular docking of *PNPLA3*_rs738409 (I148) and MT (148M) with a bioactive compound for pyranocyanin A

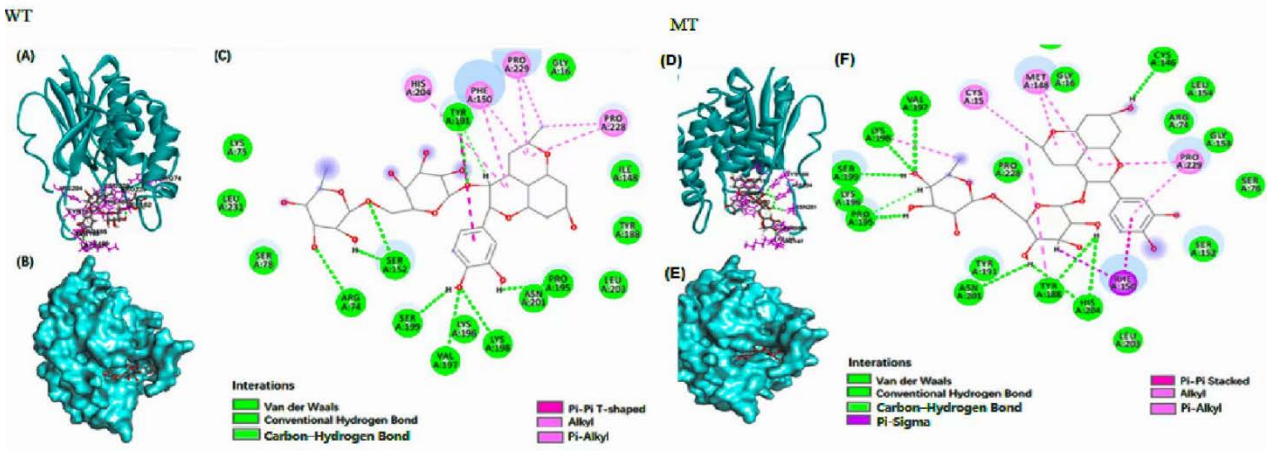

(A,D) Diagrammatic representation of the compound (ball and stick model) binding with WT and MT of *PNPLA3*, respectively. (B,E) binding of the compound at the central cavity with WT and MT of *PNPLA3*, respectively. (C,F) 2D depiction of *PNPLA3* interacting with the compound and the nature of forces involved in stabilizing–complex of bioactive compound WT and MT of *PNPLA3*, respectively. *PNPLA3*, phospholipase domain containing 3.

Figure S3. Molecular docking of *PNPLA3*_rs738409 (I148) and MT (148M) with a bioactive compound for delta-viniferin

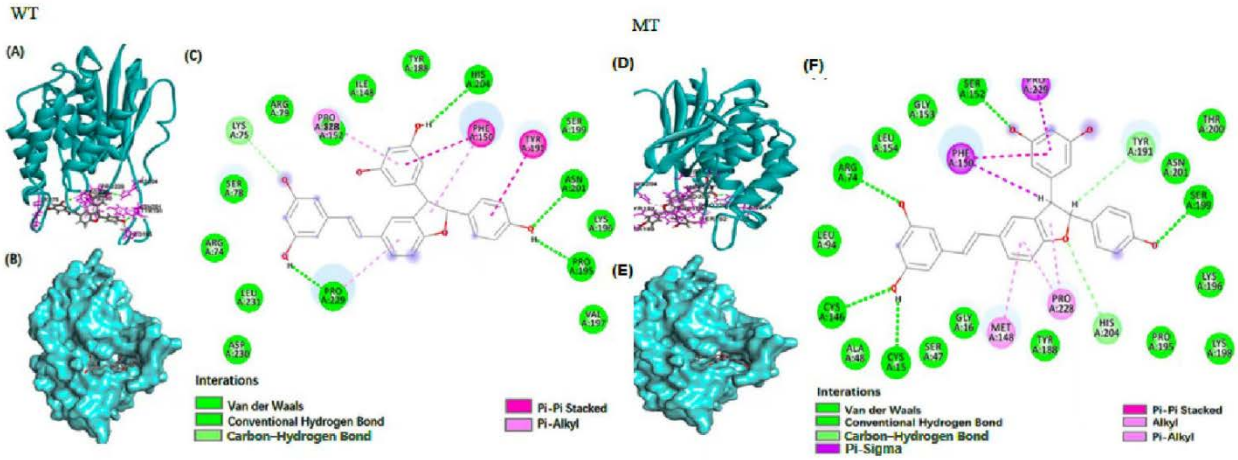

(A,D) Diagrammatic representation of the compound (ball and stick model) binding with WT and MT of *PNPLA3*, respectively. (B,E) binding of the compound at the central cavity with WT and MT of *PNPLA3*, respectively. (C,F) 2D depiction of *PNPLA3* interacting with the compound and the nature of forces involved in stabilizing–complex of bioactive compound WT and MT of *PNPLA3*, respectively. *PNPLA3*, phospholipase domain containing 3.

Figure S4. Molecular docking of *PNPLA3*_rs738409 (I148) and MT (148M) with a bioactive compound for petunidin 3-rutinoside

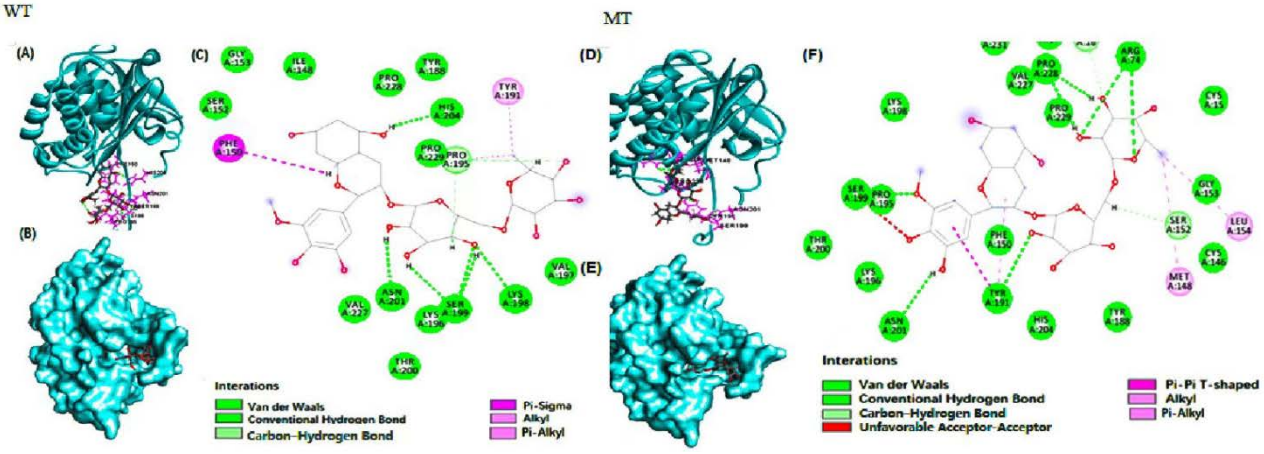

(A,D) Diagrammatic representation of the compound (ball and stick model) binding with WT and MT of *PNPLA3*, respectively. (B,E) binding of the compound at the central cavity with WT and MT of *PNPLA3*, respectively. (C,F) 2D depiction of *PNPLA3* interacting with the compound and the nature of forces involved in stabilizing–complex of bioactive compound WT and MT of *PNPLA3*, respectively. *PNPLA3*, phospholipase domain containing 3.

Figure S5. Molecular dynamics (MD) simulation of *PNPLA3*_rs738409 (I148) and MT (148M) and delphinidin 3-caffeoylglucoside interaction.

A. RMSD (root mean square deviation)

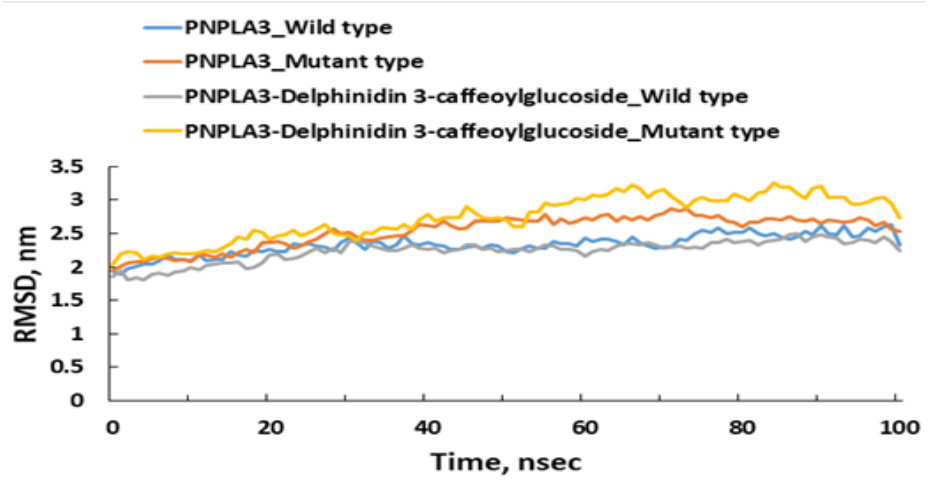

B. RMSF (root mean square fluctuation)

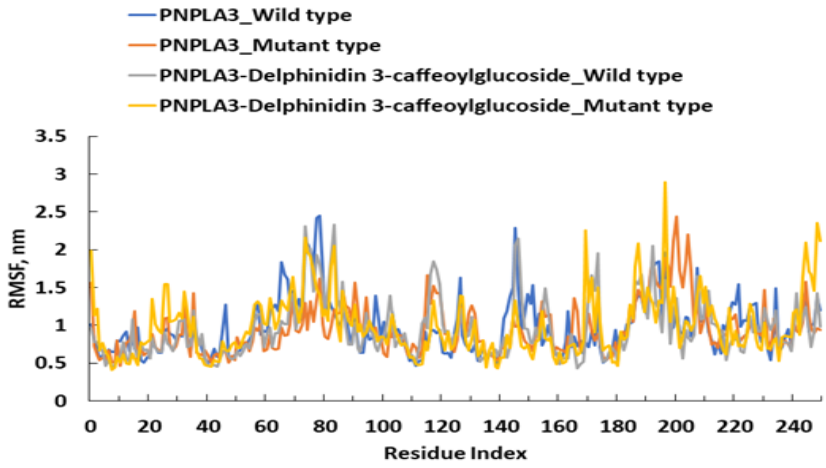

Figure S6. Molecular dynamics (MD) simulation of *PNPLA3*_rs738409 (I148) and MT (148M) and pyranocyanin A interaction.

A. **RMSD (**root mean square deviation)

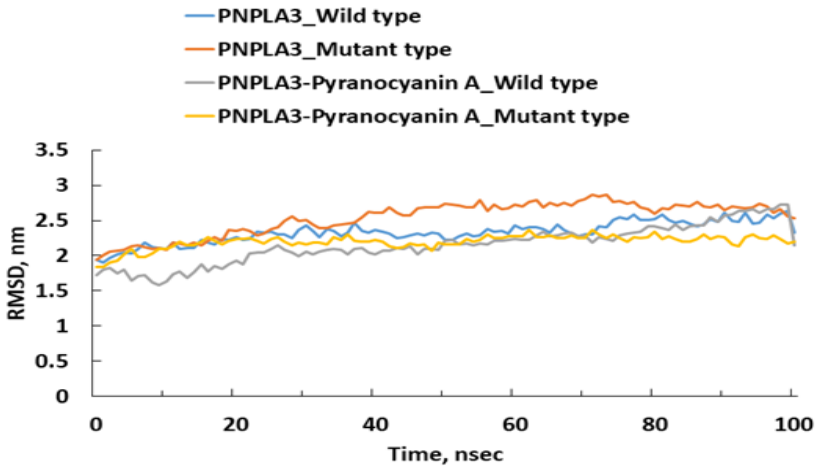

B. RMSF (root mean square fluctuation)

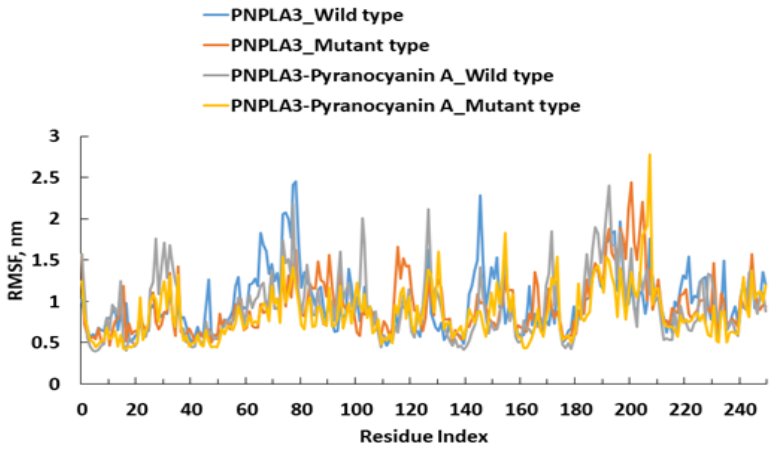

Figure S7. Molecular dynamics (MD) simulation of *PNPLA3*_rs738409 (I148) and MT (148M) and delta-viniferin interaction.

A. RMSD (root mean square deviation)

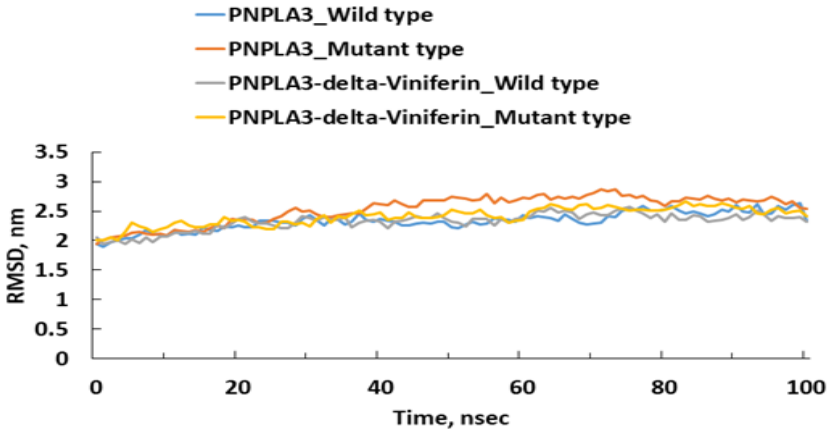

B. RMSF (root mean square fluctuation)

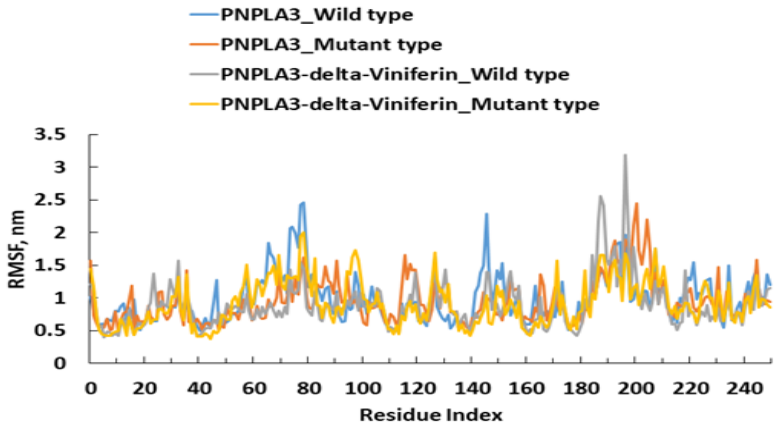

Figure S8. Molecular dynamics (MD) simulation of *PNPLA3*_rs738409 (I148) and MT (148M) and petunidin 3-rutinoside interaction.

A. RMSD (root mean square deviation)

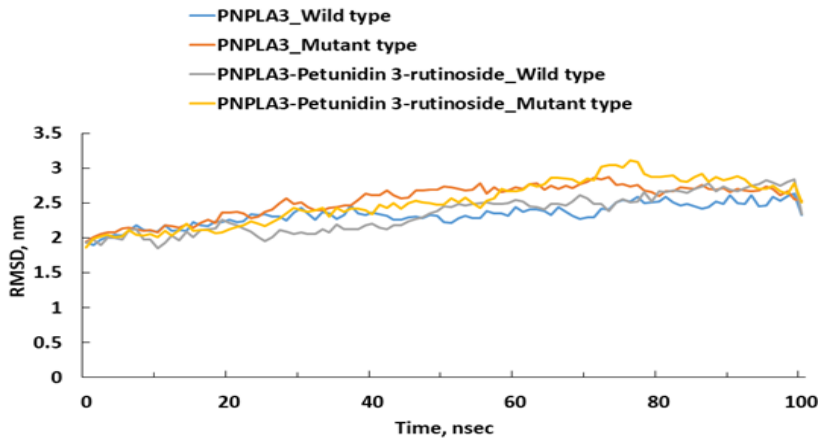

B. RMSF (root mean square fluctuation)

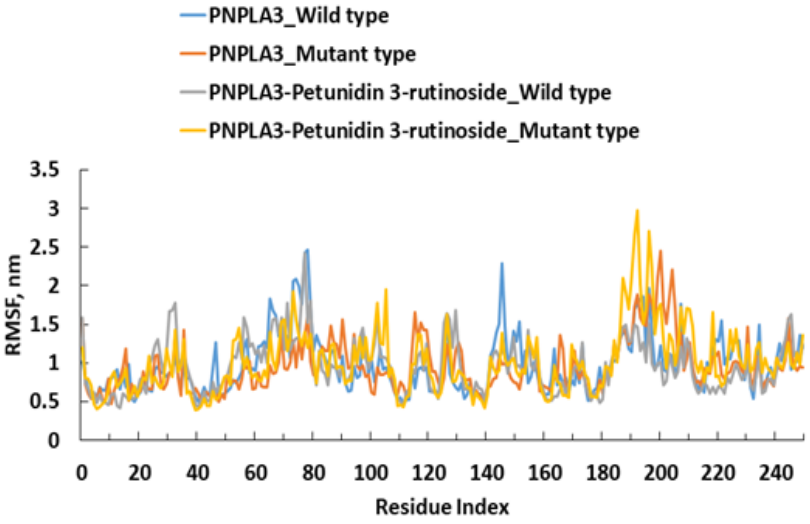

Table S1. Primer sequence used for qRT-PCR

PNPLA3	Forward:	CTGTACCCTGCCTGTGGAAT
	Reverse:	TCGAGTGAACACCTGTGAGG
SREBP-1c	Forward:	CGGAACCATCTTGGCAACAGT
	Reverse:	CGCTTCTCAATGGCGTTGT